CFD Simulation of Transverse Vibration Effects on Radial Temperature Profile and Thermal Entrance Length in Laminar Flow

Muhammad Eesa and Mostafa Barigou
School of Chemical Engineering, University of Birmingham, Edgbaston, Birmingham B15 2TT, U.K.

DOI 10.1002/aic.12243
Published online April 22, 2010 in Wiley Online Library (wileyonlinelibrary.com).

Radial heat transfer in laminar pipe flow is characterized by a wide temperature distribution over the pipe cross-section. We use a validated Computational Fluid Dynamics (CFD) model to show that the superimposition of a transverse vibration on the steady laminar flow of a Newtonian fluid moving in a pipe with an isothermal wall, generates considerable chaotic flow and radial mixing which result in a large enhancement in wall heat transfer as well as a considerably more uniform radial temperature field. Transverse vibration also causes the temperature profile to develop very rapidly in the axial direction reducing the thermal entrance length by a large factor. These effects are dependent on vibration amplitude and frequency, and fluid viscosity.
 AIChE J, 57: 51–56, 2011
Keywords: CFD, enhancement, heat transfer, temperature profile, transverse vibration

Introduction

Radial heat transfer in laminar pipe flow is governed by slow conduction which leads to a wide radial temperature distribution that poses a considerable challenge in many manufacturing processes. In continuous food sterilization, for example, the nonuniform velocity profile which characterizes viscous flow coupled with a nonuniform temperature distribution means that the coldest parts of the fluid at the centre of the pipe travel the fastest, thus resulting in a wide variation of product sterility and nutritional quality across the pipe. The challenge is to be able to sterilize the fastest parts in the core region of the pipe without over-processing the slowest parts near the wall. Increasing the temperature of the inner regions of the fluid is highly desirable so that ideally all parts of the fluid receive equal thermal treatment. Furthermore, better uniformity in the temperature profile helps reduce local variations in the fluid rheological properties which cause distortions in the velocity profile, thus making the flow behaviour of the fluid more predictable.

To improve the uniformity of the temperature distribution, methods of increasing radial mixing are required. This problem has been recognized for a long time but effective technological solutions are still missing.[1] Radial mixing can be achieved by turbulent flow conditions but the usually high fluid viscosities encountered in practice render this proposition impractical and/or uneconomical. Alternatively, the use of inline static mixers may be undesirable in hygienic processes because of the risk of contamination, for their complex geometries promote fouling and make them difficult to clean. A considerable number of studies have demonstrated the effects of pulsating flow or mechanical oscillation on the heat flux and Nusselt number in pipe flows.[2–4] However, the effects on the radial temperature distribution and the development of the thermal boundary layer in a pipe do not seem to have been reported. In this preliminary study, we use a Computational Fluid Dynamics (CFD) model to demonstrate the favourable effects that a forced transverse oscillatory

Correspondence concerning this article should be addressed to M. Barigou at m.barigou@bham.ac.uk.

wall motion can have on the radial temperature distribution, heat transfer coefficient and thermal boundary layer development in the laminar flow of Newtonian fluids in pipes.

CFD model and simulations

In this CFD model, an external sinusoidal vibrational movement is superimposed at the pipe wall in the transversal x-direction normal to the flow such that

$$x = A\sin(\omega t) \tag{1}$$

where A is the amplitude of vibration, t is time and $\omega = 2\pi f$, where f is the frequency of vibration. The linear velocity, $\dot{x}$, of the wall due to the oscillations is therefore

$$\dot{x} = \frac{dx}{dt} = A\omega\cos(\omega t) \tag{2}$$

The equations that form the basis of the CFD model are the three transport equations representing continuity, momentum, and energy for fluid flow in a pipe written in their general form as follows[5]

$$\textit{Continuity} \quad \nabla \cdot \mathbf{U} = 0 \tag{3}$$

$$\textit{Momentum} \quad \rho\frac{D\mathbf{U}}{Dt} = -\nabla p + \mu\nabla^2\mathbf{U} + \rho\mathbf{g} \tag{4}$$

$$\textit{Energy} \quad \rho C_p\frac{DT}{Dt} = \lambda\nabla^2 T + \frac{1}{2}\mu(\dot{\boldsymbol{\gamma}} : \dot{\boldsymbol{\gamma}}) \tag{5}$$

where $\mathbf{U}$ is the velocity vector, ρ is density, p is pressure, μ is Newtonian viscosity, $\mathbf{g}$ is the gravitational acceleration, C_p is specific heat capacity, T is temperature, λ is thermal conductivity, and $\dot{\boldsymbol{\gamma}}$ is shear rate. In addition, the temperature dependence of the fluid physical properties needs to be taken into account. Here, account was taken of the temperature dependence of the viscosity only, using the well-known Arrhenius model for a Newtonian fluid[6]

$$\mu = k_0\left[\exp\left(\frac{E_a}{R_G T}\right)\right] \tag{6}$$

where E_a (35,000 J mol^{-1}) is the activation energy for the viscosity of the test fluid, R_G (8.314 J mol^{-1} K^{-1}) is the gas constant, and k_0 is a pre-exponential factor. All other physical properties were assumed constant (ρ = 1000 kg m^{-3}; C_p = 4180 J kg^{-1} K^{-1}; λ = 0.668 W m^{-1} K^{-1}). The CFD model assumes that flow is Newtonian, laminar, and incompressible. The fluid is heated through the pipe wall which is held at a constant and uniform temperature. A pipe of 20 mm diameter and 400 mm length was used, which was sufficient to allow the velocity profile to fully develop and allow the fluid to receive a relatively adequate amount of heat so as to be able to clearly demonstrate the effect of vibration on the temperature profile. Using much longer pipes on the metre scale, as used in industrial installations, would excessively prolong simulation runtime; for example a 3 m pipe would typically increase the runtime from a few days to a month.

Given the short pipe length used, the problem was solved in three successive steps: (i) steady–state flow with a fixed uniform velocity $\bar{u}$ = 9.0 cm s^{-1} and a uniform temperature T_{in} = 60°C, specified at the pipe inlet; (ii) steady–state flow using as inlet boundary conditions the velocity and temperature profiles obtained at the pipe outlet from the solution of step (i); and (iii) unsteady-state flow with vibrational motion superimposed, using the complete solution along the pipe including the inlet and outlet boundary conditions from step (ii) to initiate the simulation.

The steady–state velocity profile obtained at the outlet in step (i) and used as an inlet boundary condition in steps (ii) and (iii) was fully developed. This was confirmed by the fact that the pipe length was always much larger than the hydrodynamic entrance length, L_e, given by

$$\frac{L_e}{D} = 0.05\mathrm{Re} \tag{7}$$

where D is the pipe diameter and $\mathrm{Re} = \dfrac{\rho\bar{u}D}{\mu}$ is the pipe Reynolds number.[7]

In each of these steps, a zero gauge pressure was applied at the pipe outlet. A no-slip condition and a uniform temperature of T_w = 180°C were assigned at the pipe wall in steady–state simulations; in simulations of vibrational flow, a forced oscillation was further superimposed in the transverse x-direction as described by Eq. 2.

Three-dimensional simulations were set up and executed using the commercial software package ANSYS Workbench 10.0. The geometry was meshed with tetrahedral cells. The mesh size was optimized through a mesh-independence study giving ~40 tetrahedral and prism cells across the pipe diameter and ~3000 tetrahedral cells per centimetre of pipe length. Seven inflation layers covering around 20% of the tube radius were also created near the wall to enhance mesh resolution in this region of high gradients. For a transversally moving boundary, the mesh deformation option in CFX was used allowing the specification of the motion of nodes on boundary regions of the mesh. The motion of all remaining nodes was determined by the so-called displacement diffusion model that is designed to preserve the relative mesh distribution of the initial mesh. The mesh displacement was specified using Eq. 1. Note, however, that in practice this feature is only required if the vibration amplitude is considerably larger than the mesh cell size.

The CFX code uses a finite-volume-based method to discretise the governing transport Eqs. 3, 4, and 5. The so-called "High Resolution Advection Scheme" that is intended to satisfy the requirements of both accuracy and boundedness was employed.[8] The accuracy of this scheme varies from first to second order depending on the value of the local Peclet number, so that it is as close to second order as possible without resulting in nonphysical variable values. Simulations with vibration were run in the transient mode. Each simulation was solved over the entire mean residence time of the fluid determined by the pipe length and mean flow velocity, which in this case was 4.44 s. The size of the time step was obtained by dividing the oscillation period into an optimum number of 12 equal time steps. Convergence was assumed when the root mean square (RMS) of mass, momentum, and energy residuals reached at least 10^{-3} at each time step. Most of the equations, however, generally reached RMS residual values well below the specified target.

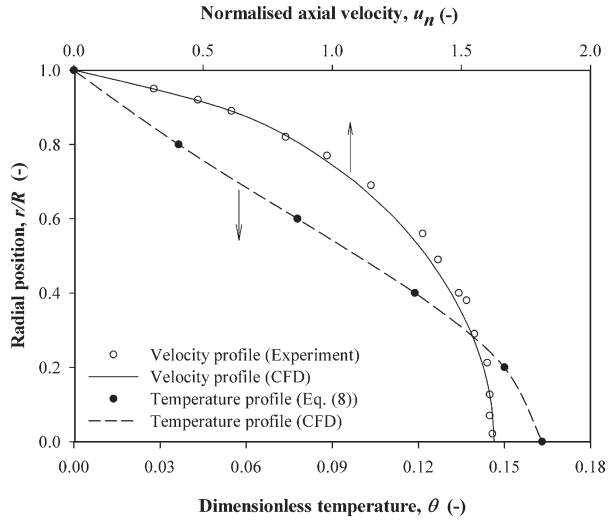

Figure 1. Validation of CFD predictions of temperature and velocity profiles in steady–state flow.

● Temperature profile for an isoviscous fluid in steady–state flow: $\mu = 1.0$ Pa s; $T_{in} = 27°C$; $T_w = 127°C$; $\bar{u} = 0.01$ m s^{-1}; ○ Velocity profile for a fluid with temperature-dependent viscosity in steady–state flow: $T_{in} = 37°C$; $T_w = 127°C$; $\bar{u} = 0.09$ m s^{-1}; $L = 1900$ mm; $\mu = \mu' \exp[-Q(T - T')/(T_w - T_{in})]$ where $Q = 1.49$, and $\mu' = 1.3$ Pa s at $T' = 25°C$ (Kwant et al.[10]).

In steady–state, on the other hand, the RMS reached 10^{-5} for all of the equations solved.

CFD validation

Though CFX, the solver component of the package ANSYS Workbench, is a generally well validated code, the CFD model was validated here as much as possible by comparing with either theoretical solutions or experimental data from the literature where possible, so as to maximize confidence in the numerical results. The steady–state flow model with heat transfer was first validated for the case of a temperature-independent viscosity. This is a textbook problem that is described by the following equation[6]

$$2\bar{u}\left[1 - \left(\frac{r}{R}\right)^2\right]\frac{\partial\theta}{\partial z} = \frac{\lambda}{\rho C_p}\left(\frac{\partial^2\theta}{\partial r^2} + \frac{1}{r}\frac{\partial\theta}{\partial r}\right) \tag{8}$$

subject to the boundary conditions

$$r = R,\ \theta = 0 \text{ for } z > 0 \tag{9}$$

$$r = 0,\ \frac{\partial\theta}{\partial r} = 0 \text{ for } z \geq 0 \tag{10}$$

$$z = 0,\ \theta = 1 \text{ for } r \leq R \tag{11}$$

where the dimensionless temperature θ is defined as $\theta = (T - T_w)/(T_{in} - T_w)$, R is the radius of the pipe, r is the radial position, and z is the axial flow direction whose origin is taken at the pipe inlet. This equation assumes that the velocity profile is fully developed but it holds in the thermal entrance region where the temperature profile is not fully developed.[6] The numerical solution of Eq. 8 was tabulated by Lyche and Bird.[9] Comparison of this solution with the CFD-predicted temperature profile for this case in Figure 1 shows an excellent agreement well within ±1%. The mean heat transfer coefficient, h, computed from CFD results also agreed with the value predicted from the above theory[6] within ± 1%.

As the variation of viscosity with temperature affects the flow field considerably, the velocity profile computed by CFD under the conditions of a temperature-dependent viscosity was also validated. The CFD predictions of the fully developed steady–state velocity profile are compared in Figure 1 with experimental measurements from Kwant et al.[10] for the same conditions of flow, showing a very close agreement between CFD and experiment with a mean difference within ±1%. It should also be noted that, in this case and in all subsequent simulations, the energy balance was always verified to a very high degree of accuracy.

CFD modeling of isothermal Newtonian and non-Newtonian flows under forced vibration, using the ANSYS-CFX code, has been validated in our recent studies.[11,12] Comparison with experimental measurements showed that the code is able to predict such complex flows with a very good accuracy. However, experimental data on vibrated nonisothermal flows are unavailable. Nonetheless, given the excellent agreement between CFD, theory and experimental results achieved in all the above validation tests, we believe that the present CFD model is sufficiently robust and reliable for the purpose of studying the effects of vibration on the heat transfer characteristics of the Newtonian flows considered here.

Results and Discussion

CFD results showed that transverse oscillations can have a substantial effect on the radial temperature distribution of the fluid accompanied by a large impact on the rate of heat transfer. The extent of these effects is governed by vibration amplitude and frequency, and fluid viscosity.

Effect of vibration amplitude and frequency

Simulations were conducted for vibration amplitudes of 1 and 2 mm and frequencies of 25 and 50 Hz, while keeping

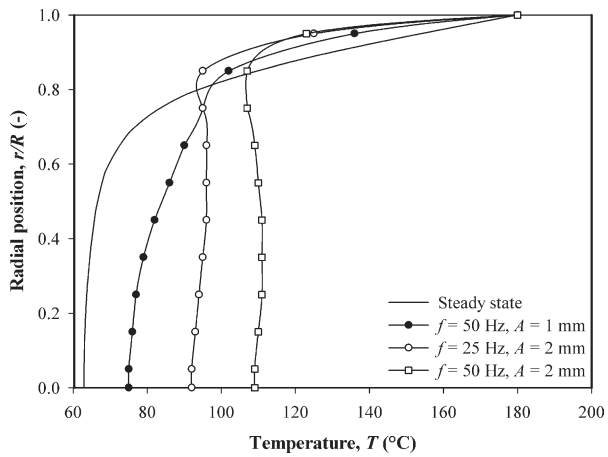

Figure 2. Effect of vibration amplitude and frequency on the mean temperature profile at the pipe exit.

$k_0 = 5 \times 10^{-7}$ Pa s; $T_w = 180°C$; $T_{in} = 85°C$; $\bar{u} = 0.09$ m s^{-1}; $L = 400$ mm.

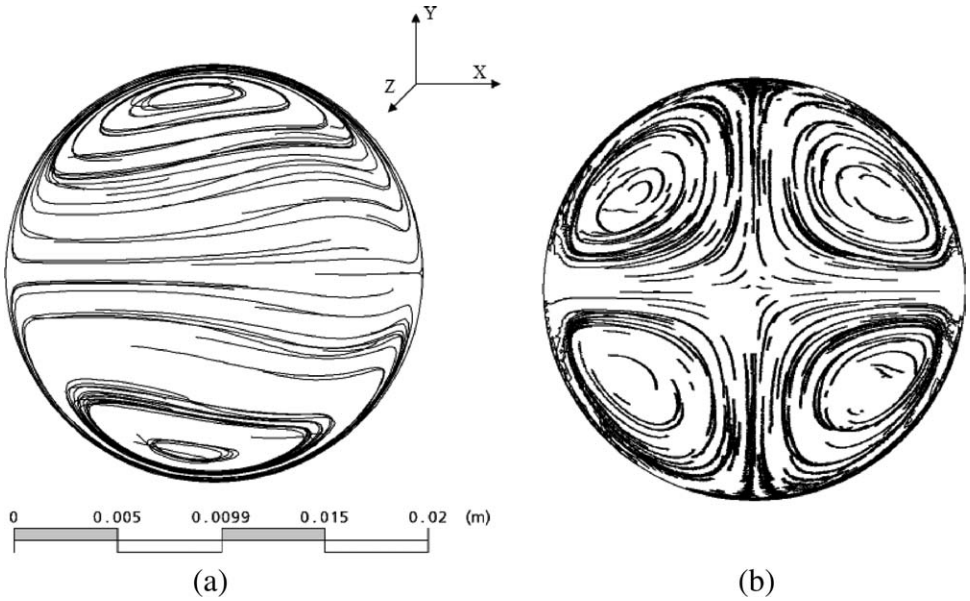

Figure 3. A sample of: (a) streamlines projected on the pipe exit plane; and (b) fluid trajectories projected on the pipe exit plane.

Note that streamlines and trajectories are not identical in unsteady flow.

all other parameters constant. The azimuthally averaged radial temperature profiles obtained at the pipe exit are compared in Figure 2 where the large effect of vibration is clearly demonstrated. In steady laminar flow, heat is transferred by conduction in the radial direction and, as a result, in this relatively short pipe only the fluid flowing near the wall is significantly heated, while the temperature of most of the fluid remains virtually at its inlet value. Transversal vibration, however, induces a considerable degree of radial mixing in the fluid. In steady–state flow the streamlines, and coinciding trajectories, are straight lines along the pipe. Vibration, however, creates a swirling or spiralling motion in the fluid, as clearly represented by the complex streamlines and fluid trajectories projected on the pipe exit plane in Figure 3. These vortical structures cause considerable chaos and radial mixing, thus, leading to a more uniform temperature distribution and a large increase in the exit temperature. This chaotic laminar flow is characterized by low values of the pipe Reynolds number and the vibrational Reynolds number,[4] $\mathrm{Re_v} = \rho A \omega D/\mu$, as shown in Table 1.

Vibration also enhances the heat transfer coefficient considerably above its steady–state value h, as demonstrated by the values presented in Table 1. The results show that increasing either A or f leads to a better temperature uniformity and a much higher heat transfer coefficient h_v. However, these effects seem to be more sensitive to A than f, as doubling the amplitude from 1 to 2 mm at $f = 50$ Hz leads to a significantly more uniform temperature profile and a greater heat transfer coefficient than doubling the frequency from 25 to 50 Hz at $A = 2$ mm.

Thermal entrance length

The effects of vibration on the development of the thermal boundary layer as represented by the thermal entrance length and temperature profile along the pipe are depicted in Figure 4. In steady laminar flow, the thermal entrance length, L_{th}, can be estimated from[7]

$$\frac{L_{\mathrm{th}}}{D} \approx 0.05 \mathrm{Re.Pr} \tag{12}$$

where $\mathrm{Pr} = C_p \mu/\lambda$ is the Prandtl number.

The steady–state temperature profile develops extremely slowly, showing hardly any change over the pipe length. In fact, under these conditions the estimated thermal entrance length would be $L_{\mathrm{th}} \sim 11$ m. The temperature map in Figure

Table 1. Comparison of Heat Transfer Coefficient for Steady and Vibrational Flows: $k_0 = 5 \times 10^{-7}$ Pa s; $T_w = 180°C$; $T_{in} = 85°C$; $\bar{u} = 0.09$ m s^{-1}; $L = 400$ mm

Vibration Frequency f (Hz)	Vibration Amplitude A (mm)	Reynolds Number* $\mathrm{Re} = \rho \bar{u} D/\mu$	Vibration Reynolds Number* $\mathrm{Re_v} = \rho A \omega D/\mu$	Prandtl Number* $\mathrm{Pr} = C_p \mu/\lambda$	Steady–State Heat Transfer Coefficient h (W m^{-2} K^{-1})	Vibrational Heat Transfer Coefficient h_v (W m^{-2} K^{-1})	Enhancement Ratio $E = h_v/h$
25	2	18	63	625	426	828	1.9
50	2	18	126	625	426	1502	3.5
50	1	18	63	625	426	671	1.6

*Calculated at the inlet temperature T_{in}.

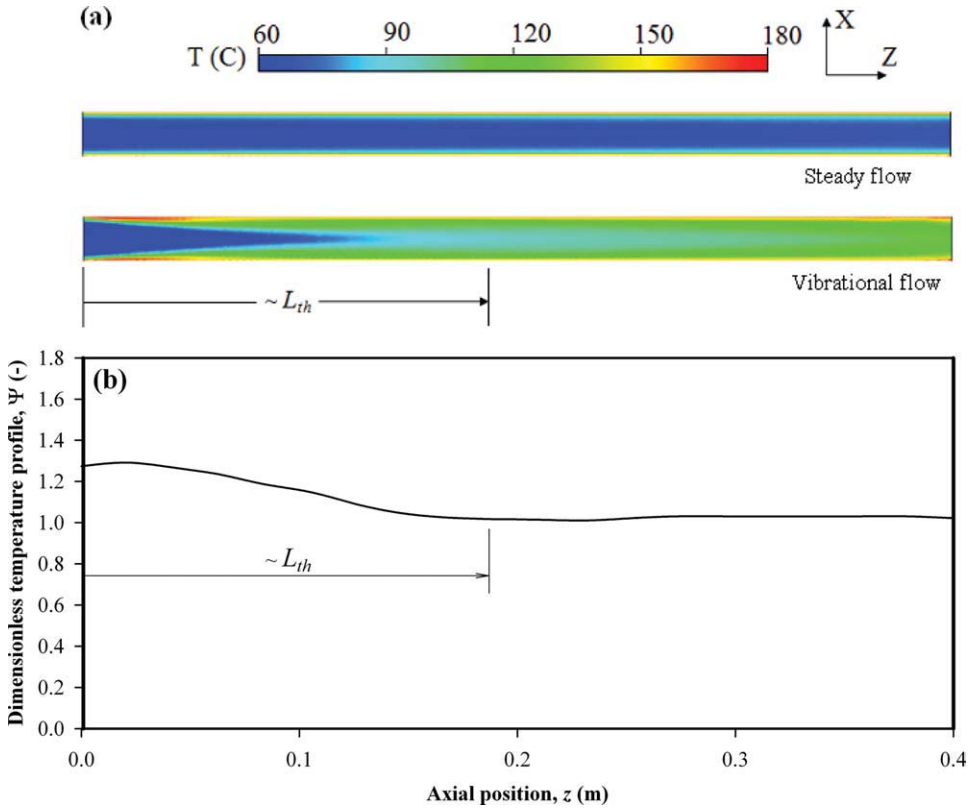

Figure 4. Effect of vibration on thermal entrance length L_{th}.

(a) Temperature map along the pipe for steady–state and vibrational flow; and (b) variation of dimensionless temperature profile along pipe centreline: $k_0 = 5 \times 10^{-7}$ Pa s; $T_w = 180°C$; $T_{in} = 85°C$; $\bar{u} = 0.09$ m s^{-1}; $A = 2$ mm; $f = 50$ Hz. [Color figure can be viewed in the online issue, which is available at wileyonlinelibrary.com.]

4 shows, however, that with vibration a very rapid development of the temperature profile takes place, which means that the full effects of the oscillations are felt in the early stages of the flow. The temperature profile is said to be thermally fully developed when the dimensionless temperature profile denoted by

$$\Psi = \frac{T_w - T(r,z)}{T_w - T_m(z)} \tag{13}$$

remains unchanged in the axial direction, i.e., $\Psi \neq f(z)$, where $T(r, z)$ is the temperature at a position (r, z) and T_m is the area-averaged fluid temperature.[7] In other words, at any fixed r position along the pipe we must have

$$\frac{\partial}{\partial z}\left(\frac{T_w - T(r,z)}{T_w - T_m(z)}\right) = 0 \tag{14}$$

The plot in Figure 4 shows the variation of Ψ along the pipe centreline which indicates that a fully developed thermal profile is achieved in the vibrated flow over a relatively very short length. Thus, it appears that the thermal entrance length can be reduced by at least an order of magnitude compared with its value in steady–state flow.

In practice, the application of a forced vibration to long pipes would mean that a substantial enhancement in heat transfer characteristics can be achieved by using frequencies and amplitudes significantly lower than those employed in this study. The implications of these results are of practical significance for processes where a uniform temperature profile is needed, such as in food sterilization. The temperature of the fluid layers adjacent to the wall can be reduced, thus avoiding overheating, while the temperature at the pipe centre can be increased rapidly to achieve sterility. These two effects should in principle reduce the loss in product quality that usually arises from over-processing.

Effect of fluid viscosity

Initial results show that the fluid viscosity is one of the key parameters governing the observed effects. The effects of vibration on the uniformity of the temperature profile and on the heat transfer coefficient are more significant for less viscous fluids, as demonstrated in Figure 5. As would be expected, a lower viscosity promotes fluid mixing, and therefore facilitates a more uniform temperature distribution and better radial heat transfer. However, preliminary results suggest that even more viscous fluids than those considered here can be positively affected by using a judicious choice of vibration amplitude and frequency.

Conclusions

Forced transverse vibration has positive benefits for heat transfer in laminar flow under conditions of an isothermal pipe wall: a much more uniform radial temperature profile, a

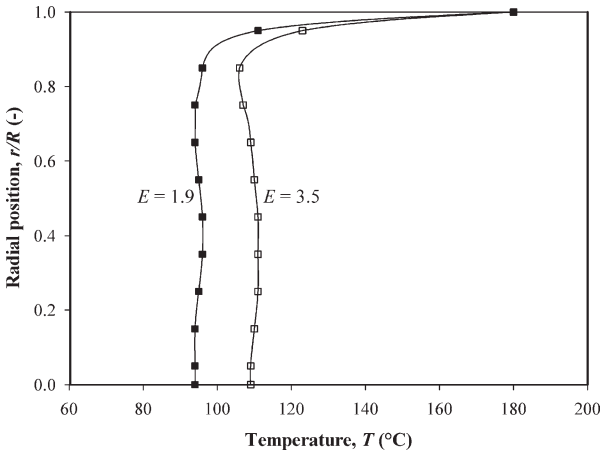

Figure 5. Effect of viscosity on the mean temperature profile at the pipe exit.

■ μ at inlet = 1.0 Pa s; □ μ at inlet = 0.1 Pa s. T_w = 180°C; T_{in} = 85°C; $\bar{u}$ = 0.09 m s^{-1}; A = 2 mm; f = 50 Hz; L = 400 mm. E, heat transfer enhancement ratio, is defined in Table 1.

rapid development in the temperature profile along the pipe, and a substantial increase in radial heat transfer. These effects are governed by the amplitude and frequency of vibration so that higher amplitudes and frequencies lead to better improvements in heat transfer characteristics. More viscous fluids require a more energetic vibration but the effects appear to be more sensitive to the amplitude than the frequency of oscillation. More detailed work is needed to systematically investigate the role of these variables and of other key rheological parameters when more complex fluids of non-Newtonian rheology are considered. It is also plausible that in practice the vigorous spiralling fluid motion generated by a forced vibration would have further benefits in reducing fouling in the pipe because of the energetic cleaning action that the fluid motion would create at the wall. Moreover, in a solid-liquid flow vibration may also help keep particles in suspension, thus, enhancing homogeneity in heat transfer to both the continuous and dispersed phase.

Literature Cited

1. Jung A, Fryer PJ. Optimising the quality of safe food: computational modelling of a continuous sterilisation process. *Chem Eng Sci*. 1999;54:717–730.
2. Gündoğdu MY, Çarpinlioğlu MÖ. Present state of art on pulsatile flow theory part 1: laminar and transitional flow regimes. *JSME Int J*. 1999;42:384–397.
3. Klaczak A. Report from experiments on heat transfer by forced vibrations of exchangers. *Heat Mass Trans*. 1997;32:477–480.
4. Lee YH, Chang SH. The effect of vibration on critical heat flux in a vertical round tube. *J Nucl Sci Technol*. 2003;40:734–743.
5. Bird RB, Armstrong RC, Hassager O, Curtiss CF. *Dynamics of Polymeric Liquids*, vol. 1: *Fluid Mechanics*, 2nd ed. New York, USA: Wiley, 1987.
6. Tanner RI. *Engineering Rheology*. Oxford: Clarendon Press, 1985.
7. Çengel YA. *Heat Transfer: A Practical Approach*. McGraw Hill Professional, 2003.
8. Barth TJ, Jesperson DC. The design and application of upwind schemes on unstructured meshes. *AIAA*. 1989.
9. Lyche BC, Bird RB. The Graetz-Nusselt problem for a power-law non-Newtonian fluid. *Chem Eng Sci*. 1956;6:35–41.
10. Kwant PB, Fierens RHE, Van Der Lee A. Non-isothermal laminar pipe flow–II. Experimental. *Chem Eng Sci*. 1973;28:1317–1330.
11. Deshpande NS, Barigou M. Vibrational flow of non-Newtonian fluids. *Chem Eng Sci*. 2001;56:3845–3853.
12. Eesa M, Barigou M. CFD analysis of viscous non-Newtonian flow under the influence of a superimposed rotational vibration. *Comput Fluids*. 2008;37:24–34.

Manuscript received Apr. 9, 2009, revision received Aug. 12, 2009, and final revision received Feb. 26, 2010.